Active Vibration Control of a Wind Turbine Blade Using Synthetic Jets

Victor Maldonado[1], Matthew Boucher[2], Rebecca Ostman[1] and Michael Amitay[1,*]
[1]Mechanical, Aerospace, and NuclearEngineering Department
[2]Electrical, Computer, and Systems Engineering Department
Rensselaer Polytechnic Institute, Troy, NY 12180, USA

Active vibration control via an array of synthetic jet actuators was investigated experimentally in a wind tunnel. Using synthetic jets the flow over a small scale S809 finite wind turbine blade was controlled, resulting in reduction of the blade's structural vibrations. The effectiveness of the synthetic jets was explored for a range of post-stall angles of attack at Reynolds numbers between 7.1×10^4 and 2.38×10^5. The blade vibrations were measured and quantified using a pair of strain gauges mounted at the root of the model. Using flow control, significant vibration reduction was observed for some post-stall angles of attack. A correlation between vibration reduction and the degree of flow reattachment, measured using Particle Image Velocimetry, was found.

1. INTRODUCTION

As wind turbines become larger, there becomes an increasing interest to develop methods to reduce blade loads, and consequently, structural vibration that directly impacts the life and cost of operation of the turbine. There are primarily two control methods to keep blade loads within acceptable limits. Stall regulation maintains the blade pitch fixed and operates the turbine at a near constant rotational speed. As the wind speed increases, the angle of attack increases causing the blades to eventually stall resulting in a decrease in lift and an increase in drag, yielding a lower tangential load. The other more effective method to reduce blade loads utilized in modern wind turbines is variable rotational speed and individual blade pitch control, whereby a large actuator mechanism is connected to each blade and controlled independently. In addition to regulating blade loads, individual blade control is principally used to limit output power and torque in above-rated wind speeds in order to keep turbine operation within its design limits. While this type of control method has the ability to respond sufficiently to changing wind speeds (due to blade rotation) and thus asymmetric aerodynamic loading at each blade at a relatively slow once-per-revolution manner, it cannot respond to higher frequency atmospheric phenomena such as turbulence, wind gusts, and wind shear. Gusts can result in a sudden increase in the blade effective angle of attack, which can yield high unsteady loads on the blade leading to structural failures. These loads are often unavoidable due to the slow response of conventional pitch control actuators in decreasing the angle of attack; hence the development of locally distributed high bandwidth flow control actuators with built in intelligence embedded on the blades is needed.

In recent years, there have been numerous studies on the application of active flow control with piezobimorph actuators and/or MEMS (Micro Electrical Mechanical Systems) for active performance enhancement, including load and vibration reduction of wind turbine blades. Most of these studies aim at the feasibility of manipulating aerodynamic loads using such actuators attached to control surfaces (typically near the trailing edge of the blade) commonly referred to as flaps, microtabs, etc. The use of microtabs as aerodynamic devices for load control on wind turbine blades has been extensively investigated by van Dam[1–4], where active micro tabs deployed near the trailing edge on the suction surface of a blade have the ability to reduce the lift and therefore loads on the blade. Wingerden et al.[5] showed a proof of concept study of a 'smart' 3-D rotor blade with trailing edge flaps and a feedback controller for load control. Research on this topic has also been performed in the wind industry where trailing edge flaps[6–12] and MEMS tabs[13] have been used for load alleviation including their feasibility on a rotating blade, Buhl et al[12].

The field of active flow control in general (including the use of piezoelectric driven synthetic jets and blowing and suction mechanisms) is not new, and has generated an extensive amount of research

* Corresponding author, e-mail: amitam@rpi.edu

findings where most of the focus has been largely on control of separation. Separation control using synthetic jets has recently been demonstrated as a viable means to reduce wind turbine blade structural vibration (Maldonado et al.[14]) by exploiting the narrow-band receptivity of the separating shear layer and the upstream boundary layer to external actuation. Previously, Oster and Wygnanski[15] and Roberts[16] showed that the actuation can affect the global flow field by modifying the evolution and interactions of the large-scale vortical structures. These modifications can lead to a Coanda-like deflection of the separating shear layer towards the surface[17] such that the layer vortices are advected downstream in close proximity to the surface.

This approach has been implemented, with varying degrees of success and different actuation means, to restore aerodynamic performance of stalled airfoils and flaps.[18–20] In particular, Seifert et al.[20] and Wygnanski[21] argued that the actuation is most effective when its period scales with the advection time over the length of the flow domain downstream of separation as measured by the reduced frequency, F^+. Therefore, when the separation domain scales with the characteristic length of an aerodynamic body, the (dimensionless) actuation frequency can couple to, and even drive the shedding frequency in the near wake. The possibility of coupling between (nominally) time-periodic shedding of coherent vortices and the separated shear layer in the absence of actuation is intriguing because such feedback between the near wake instabilities and the separating shear layer is even more pronounced in the presence of actuation; thereby amplifying the unsteady component of the global aerodynamic forces. The approach of coupling the actuation frequency to instabilities relies explicitly on the narrow-band receptivity of the separating shear layer to a control input that is effective within a limited spatial domain immediately upstream of separation. Furthermore, when the flow is not separated the effectiveness of this approach diminishes.

Another approach to control the flow is based on fluidic modification of the apparent aerodynamic shape of lifting surfaces using integrated synthetic jets that are driven at high frequencies (i.e., much larger than the characteristic frequencies of the flow); this approach was presented by Amitay & Glezer.[22] Thus, it does not necessarily rely on coupling to global flow instability and therefore can be applied over a broader range of flow conditions.[23,24] Furthermore, this approach can accommodate broader band control algorithms when more complex actuation waveforms are used such as the pulse modulation technique.[25,26] Earlier work[26] has demonstrated that flow separation at high angles of attack can be mitigated or altogether suppressed by appropriate dynamic tailoring of the apparent surface curvature (and thus the distribution of the streamwise pressure gradient) in advance of the onset of separation.

1.1 Motivation and Objectives

The majority of the literature concerning wind turbine blade load and vibration reduction using blade distributed active flow control techniques deals with the deflection or deployment of aerodynamic control surfaces. However, these techniques can be overly mechanically complex to implement and/or not very efficient, i.e. the power needed to apply the control is of the same magnitude as the improvement. The objective of the present paper is to reduce a wind turbine blade model's structural vibration by efficiently controlling the blade's aerodynamic characteristics selectively along its span for a range of blade pitch angles. This will be accomplished by spatially distributed arrays of mechanically simple, low power consumption synthetic jets near the leading edge for separation control, which in turn affects vibration due to suppression of the separating boundary layer. It is noteworthy that the methodology presented in this paper can be accomplished using various types of actuators; however, it is believed that synthetic jets are the simplest, most efficient, cheapest and the most matured for wind turbine applications.

Reduction of vibration can help increase the lifetime of the blades, and it is an enabling technology that promotes the development of longer blades needed to capture more wind energy (e.g., off-shore wind turbines). The synthetic jet flow control system is integrated on these blades and is designed to work in parallel to conventional pitch actuators, but at a much higher bandwidth, making them effective in responding to gusts and other higher frequency atmospheric phenomena as mentioned earlier. This approach has the potential to reduce the size of conventional pitch actuators, and the distributed nature of the jets also has the ability to shed the excess lift from selected portions of the blade (this approach was examined by DeSalvo & Glezer[27] on 2-D airfoils with promising results).

2. EXPERIMENTAL METHODOLOGY

The feasibility of vibration reduction on an airfoil section using a piezoelectric synthetic jet based flow control system was demonstrated on a finite span NACA 4415 blade model (Maldonado et al.[14]). It was crucial to determine if the same performance could be achieved on an airfoil section representative of

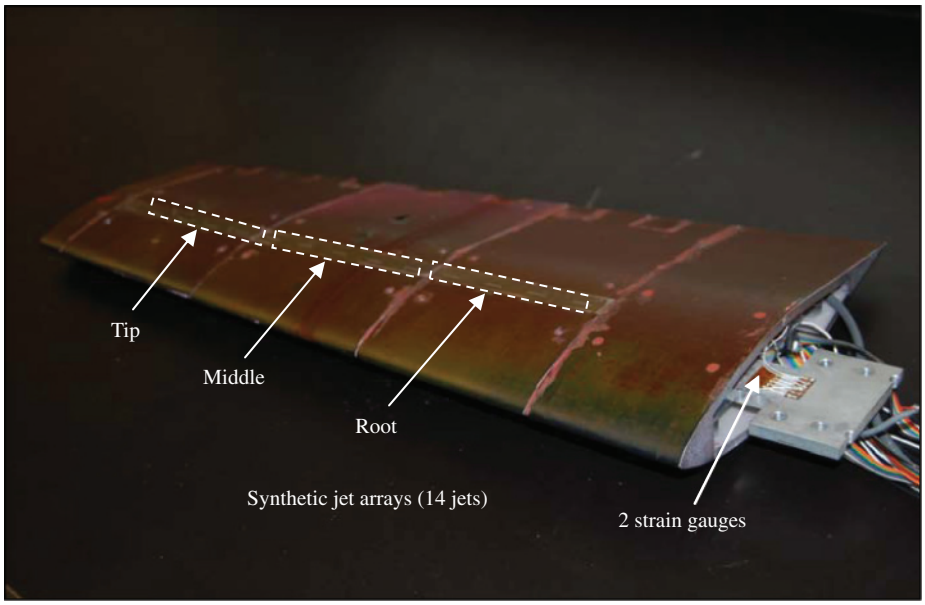

Figure 1. S809 wind turbine blade model Schematic

full-scale wind turbines currently in operation. In the present experiments, a 3-D configuration finite-span (b = 0.457 m) with a cross-section shape S809 airfoil wind turbine blade model was designed and manufactured using stereolithography techniques (see Figure 1). The blade has a taper ratio, C_t/C_r, of 0.688, where C_t and C_r are the tip and root chords, respectively (C_r = 0.203 m). The modular design allowed for independent access to three spanwise arrays of synthetic jets (14 jets total). A schematic of a synthetic jet is shown in Figure 2.

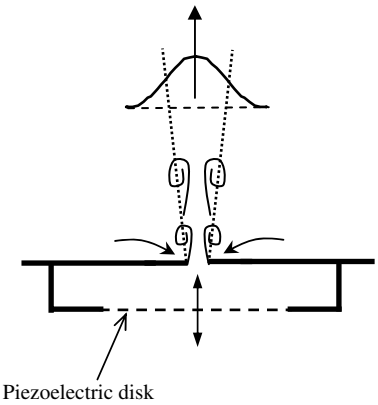

Figure 2. Schematics of the synthetic jet

The synthetic jet based flow control system consists of 14 spatially distributed synthetic jets located at a chord-wise location of C_j/C_r = 0.318. Each synthetic jet has a rectangular orifice parallel to the blade taper and with a width of 0.75 mm and a length of 10 mm and are spaced 25.40 mm apart. Each synthetic jet is individually controlled and is driven with a 20 mm piezo disk with a sinusoidal actuation frequency of f_{act} = 2100Hz. Note that the range of characteristic frequencies of the flow over the model is 64Hz to 175Hz (based on the "time of flight" over the mean chord, for free stream velocities of 11 m/s to 30 m/s, respectively). This range of velocities was selected to ensure that the corresponding characteristic frequencies of the flow would be about equal to or less than one order of magnitude compared to the actuation frequency, and thus enable the use of different actuation waveforms and provide adequate flow control effectiveness.

The strength of the synthetic jets (relative to the free stream velocity) is quantified using the momentum coefficient, C_μ, defined as:

$$C_\mu = \frac{n\bar{I}_j}{\frac{1}{2}\rho U_\infty^2 A_w} \tag{1}$$

where U_∞ is the free stream velocity, A_w is the blade area, ρ is the density, and n is the number of synthetic jets activated. $\bar{I}_j$ is the time-average jet momentum calculated only during the blowing portion of the cycle, defined as:

$$\bar{I}_j = \frac{1}{\tau}\rho A_{sj}\int_0^\tau u_j^2(t)\,dt \tag{2}$$

where τ is the synthetic jet outstroke time, A_{sj} is the area of the synthetic jet orifice, and $u_j(t)$ is the centerline velocity at the jet exit plane. The time-average jet moment is defined only for the outstroke part of the cycle. For the experiments presented in this paper, the momentum coefficient range was $1.34 \times 10^{-3} < C_\mu < 5.97 \times 10^{-3}$.

2.1 Experimental Setup and Instrumentation

The experiments were conducted in an open-return low speed wind tunnel currently operating at RPI. The test section has an 80 cm × 80 cm cross-section and is 5 m long. The wind tunnel is capable of achieving speeds up to 50 m/s and a turbulence level of less than 0.25%. The wind turbine blade model was mounted to one of the sidewalls of the test section on a pitch actuator capable of generating static blade pitch angles of attack, as well as unsteady angle of attack motions by prescribing a dynamic pitch waveform. The motion controller was implemented in xPC Target, a real-time operating system from Mathworks for control development. The blade pitch actuator is a DC-motor based system with an optical encoder for position feedback, enabling angular position to 0.01 degrees.

The blade model was instrumented with a pair of strain gauges to measure blade structural vibration by quantifying its unsteady tip deflection. The strain gauges were surface mounted on the upper and lower surface of the blade's aluminum spar near the root. This created a Wheatstone half-bridge, where each gauge produced an equal but opposite magnitude strain, resulting in improved resolution of the strain reading. The strain gauges were oriented in the spanwise direction to capture the bending movements of the model (i.e., the deflections that are correlated to the roll moment). The voltage output from the strain gauges due to spanwise bending was correlated to the deflection at the tip. First, the voltage output was calibrated to the tip deflection by manually loading the blade with multiple equal weights (at the tip) and measuring its deflection. A second order curve of the tip deflection as a function of voltage was then fitted to the data points and was integrated into the code to generate the time histories of the tip deflection.

The flow field over the suction surface of the blade was measured using Particle Image Velocimetry (PIV) at a spanwise location of $y/b = 0.47$ (about mid span) coinciding with the middle of a synthetic jet orifice to capture maximum flow control effectiveness. The PIV system consists of a 1376 × 1040 pixel resolution thermo-electrically cooled 12-bit CCD camera, a pair of pulsed 120 mJ Nd:YAG lasers, and a programmable timing unit. In the present experiments, 2-D PIV data was acquired where the CCD camera was mounted on a computer-controlled three-axis traverse. The laser light sheet was emitted from a free-moving optical arm and a laser head with variable lenses that can be positioned at any location along the outside of the test section. With this arrangement, precise positioning of the laser light sheet was obtained. A smoke generator (model Magnum 800 made by Martin Manufacturing PLC) was used together with water-based fluid to provide droplets on the order of a few μm in diameter to serve as flow tracers. The smoke was introduced into the tunnel via the wind tunnel fan's air filter. The streamwise and cross-stream velocity components (U, V) were computed from the cross-correlation of pairs of successive images with 50% overlap between the interrogation domains. For the time-averaged velocity vector fields, 250 image pairs were processed using an advanced multi-pass method where the initial and final correlation passes were 64 × 64 pixels and 32 × 32 pixels, respectively. The camera was mounted at a perpendicular distance of approximately 1m to the laser light sheet, such that the distance between pixels is up to 125 μm. The maximum velocity (30.48 m/s) corresponds to an average displacement of approximately 8 pixels with an error of ±0.1pixels, which corresponds to a maximum error of ±1.25% of the free-stream velocity (±0.38m/s at the maximum speed).

Several free stream velocities were tested between 9m/s and 30m/s resulting in mean aerodynamic chord Reynolds numbers between Re_{U_∞} = 71,000 and 238,000. The Reynolds number is defined as:

$$Re_{U_\infty} = \frac{U_\infty \cdot c}{\nu} \tag{3}$$

where U_∞ is the free stream velocity, $\bar{c}$ is the mean aerodynamic chord of the blade and ν is the kinematic viscosity.

3. RESULTS

The effect of flow control on the structural vibrations of the wind turbine blade was investigated using strain gauges and PIV techniques. In the first section, the effectiveness of the synthetic jets in reducing vibrations under static conditions is explored. The section presents the global flow field measurements to provide means to understand the reduction of the structural vibration due to the flow control. The flow field measurements were acquired for a range of post-stall angles of attack between 15° and 17.5°.

3.1 Vibration Control

Without flow control, at high angles of attack, the flow separates from the surface of the blade, forming vortical structures next to the surface of the blade, which excite the blade at its structural resonance frequency. When flow control is applied, the separation is either reduced or completely mitigated, and thus reduces (or mitigates altogether) the formation of the vortical structures. The mitigation of blade structural vibration is fundamentally correlated to the extent of flow re-attachment (for a stalled blade at post-stall angles of attack) as a result of synthetic jet actuation.

The effect of the synthetic jets on the structural vibration is presented in Figure 3 at a Reynolds number of 1.85×10^5 and angle of attack of $\alpha = 16.5°$. The time histories of the blade tip deflection with and without flow control are presented. For the controlled case, the momentum coefficient of each synthetic jet is $C_\mu = 5.97 \times 10^{-3}$, where all 14 synthetic jets were activated together. Without flow control, the blade vibrates at its fundamental structural resonance frequency (f_{struc}) of around 6Hz about its mean tip deflection of ~3.25 mm. When the synthetic jets were activated the tip vibration is reduced by a factor of ~6.5.

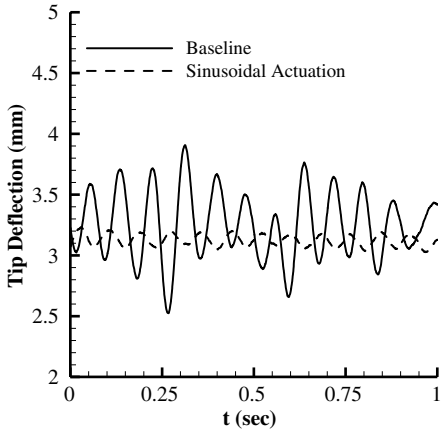

Figure 3. Unsteady tip deflection. $\alpha = 16.5°$, $Re = 1.85 \times 10^5$, and $C_\mu = 5.97 \times 10^{-3}$

The effect of flow control on the structural vibration was also evaluated by computing the power spectral density (PSD) content of the blade tip deflection, as shown in Figure 4. Without flow control, there is a noticeable peak at the structural frequency, f_{struc} of the blade. Using actuation, there is a reduction in all frequencies below 30Hz. Furthermore, the magnitude of the structural peak decreases about an order of magnitude from the baseline level. This implies that the energy associated with the structural frequency vibration of the blade has greatly reduced.

Another aspect of flow control is the ability to achieve proportional control of the blade tip deflection. This can be obtained by varying the momentum coefficient of the synthetic jets (i.e., their

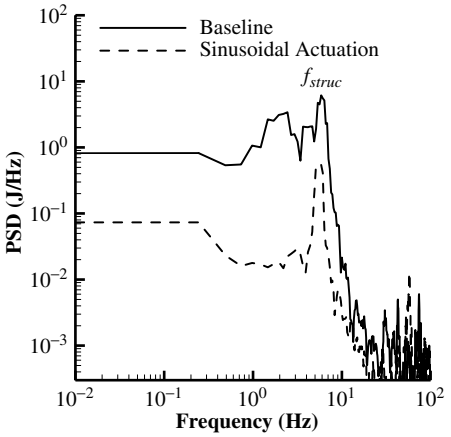

Figure 4. PSD of the structural vibration. $\alpha = 16.5°$, $Re = 1.85 \times 10^5$, and $C_\mu = 5.97 \times 10^{-3}$

strength). Figure 5 presents the effect of the momentum coefficient on the PSD structural peak, where all the synthetic jets were activated. The figure clearly shows that proportional control of the tip deflection is achieved by simply varying the momentum coefficient.

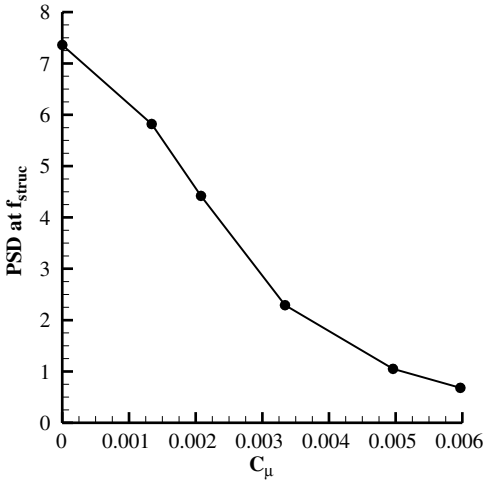

Figure 5. PSD at f_{struc} vs. synthetic jet momentum coefficient. $\alpha = 16.5°$ and $Re = 1.85 \times 10^5$

As was mentioned above, the synthetic jets were grouped in three spanwise sections: tip, middle, and root. The effect of actuating each section by itself was also investigated and is presented in Figure 6. These sections, consist of 5 jets (tip), 5 jets (middle), and 4 jets (root), are located at spanwise locations (distance from the root normalized with blade span) of $y/b = 0.167$ to 0.389, 0.389 to 0.667, and 0.667 to 0.944, respectively. The synthetic jet momentum coefficient, C_μ was 2.13×10^{-3} for the mid and tip sections (due to an equal number of synthetic jets) while for the root section, it was 20% less due to only actuating 4 jets. The Reynolds number and angle of attack was held constant at 1.85×10^5 and 16.5°. Figure 6a presents the time history of the blade tip deflections for the baseline case and 4 actuation cases: root only, middle only, tip only, and all three sections (RMT) together, while Figure 6b shows the corresponding RMS values of the tip deflection as a function of the spanwise location of the actuation. The baseline case was discussed earlier and is presented here as a reference. Actuating the root section of the blade ($y/b = 0.167$ to 0.389; 22% of blade span) results in a minor decrease of the mean amplitude to 0.14mm. Actuating only the middle section ($y/b = 0.389$ to 0.667, 27.8% of blade span) significantly decreases the mean amplitude to 0.07mm, while actuating the tip section by itself ($y/b = 0.667$ to 0.944, 27.5% of blade span) results in the largest decrease of the tip RMS (to 0.041 mm). By actuating only the tip section of the blade, the mean amplitude tip deflection is reduced by about 6.5 times. More

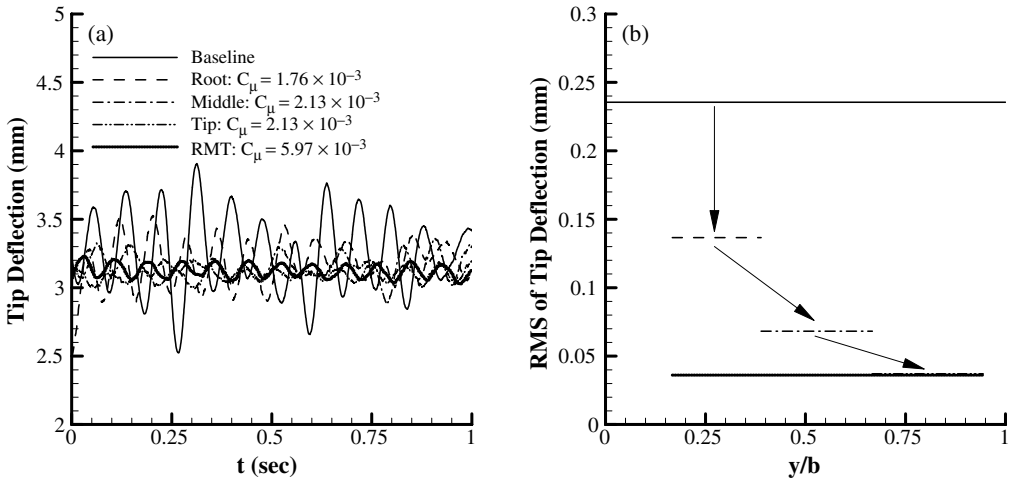

Figure 6. Effect of spanwise actuation location at $Re = 1.85 \times 10^5$ and $\alpha = 16.5°$ on (a) the unsteady tip deflection and (b) the RMS of the tip deflection at the structural frequency

profoundly however, this results in almost the same level of vibration reduction achieved by actuating all three arrays of synthetic jets simultaneously, as indicated by the dotted RMT case. Thus, actuating only the tip deflection yield similar effect as activating all three sections but with input energy savings of 64%. This result may be explained in part by the three dimensionality of the flow around a tapered finite wing, where the increasing spanwise component of the flow near the tip makes the flow more susceptible to separation in comparison to inboard regions of the blade. Thus, any actuator induced flow-reattachment that occurs near the tip will have a greater effect in mitigating tip deflection amplitude due to increased force leverage from the blade root.

The range of angles of attack under which synthetic jet actuation is effective in reducing structural vibrations was also explored and is presented in Figure 7. Here, the synthetic jet momentum coefficient was 5.97×10^{-3}, where the root, middle, and tip sections were activated together. Without flow control, the RMS levels of the tip deflections increase as the angle of attack is increased (except at $\alpha = 17.5°$). With flow control, the magnitude of the RMS tip deflection for $\alpha = 15°$ is very similar to the baseline case, presumably because the flow is still attached to the blade surface. As the angle of attack increases, the actuation results in relatively low tip deflection amplitudes below 0.05mm up to $\alpha = 16.5°$, before increasing sharply to 0.258 mm at $\alpha = 17.5°$. For angles of attack higher than 17.5°, synthetic jet actuation (located at about the quarter chord of the blade) is not effective in reducing vibration. This is explained in the next paragraph, discussing the effect of the synthetic jets on the flow field around the blade.

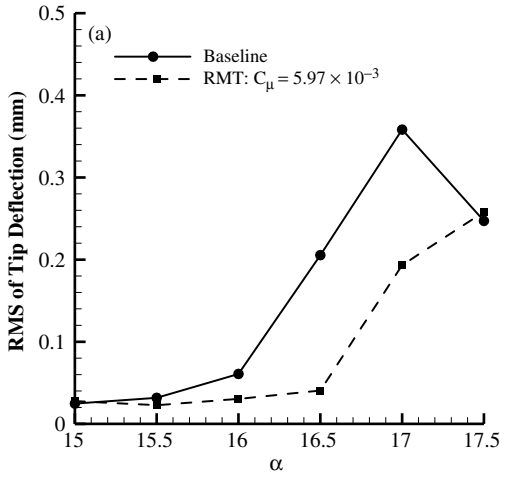

Figure 7. RMS tip deflection as a function of the blade's angle of attack at $Re = 1.85 \times 10^5$.

3.2 Flow Field Measurements

As mentioned above, activation of the synthetic jets yields profound effects on the blade's vibrations. It was speculated that it might be due to the effect of the jets on the global flow field around the blade. In order to validate this hypothesis, PIV measurements were conducted and are presented in Figures 8 and 9 for the baseline and forced ($C_\mu = 5.97 \times 10^{-3}$) cases, respectively. The PIV plane was placed at y/b = 0.47, in the middle of a synthetic jet orifice for maximum control effectiveness. Figures 8 and 9 present superimposed spanwise vorticity contours and streamlines for α = 15°, 15.5°, 16°, 16.5°, 17°, and 17.5°. Without flow control, the streamwise and cross-stream extent of the separated flow increase as the angle of attack increases, which explains the increase of the RMS tip deflection with angle of attack.

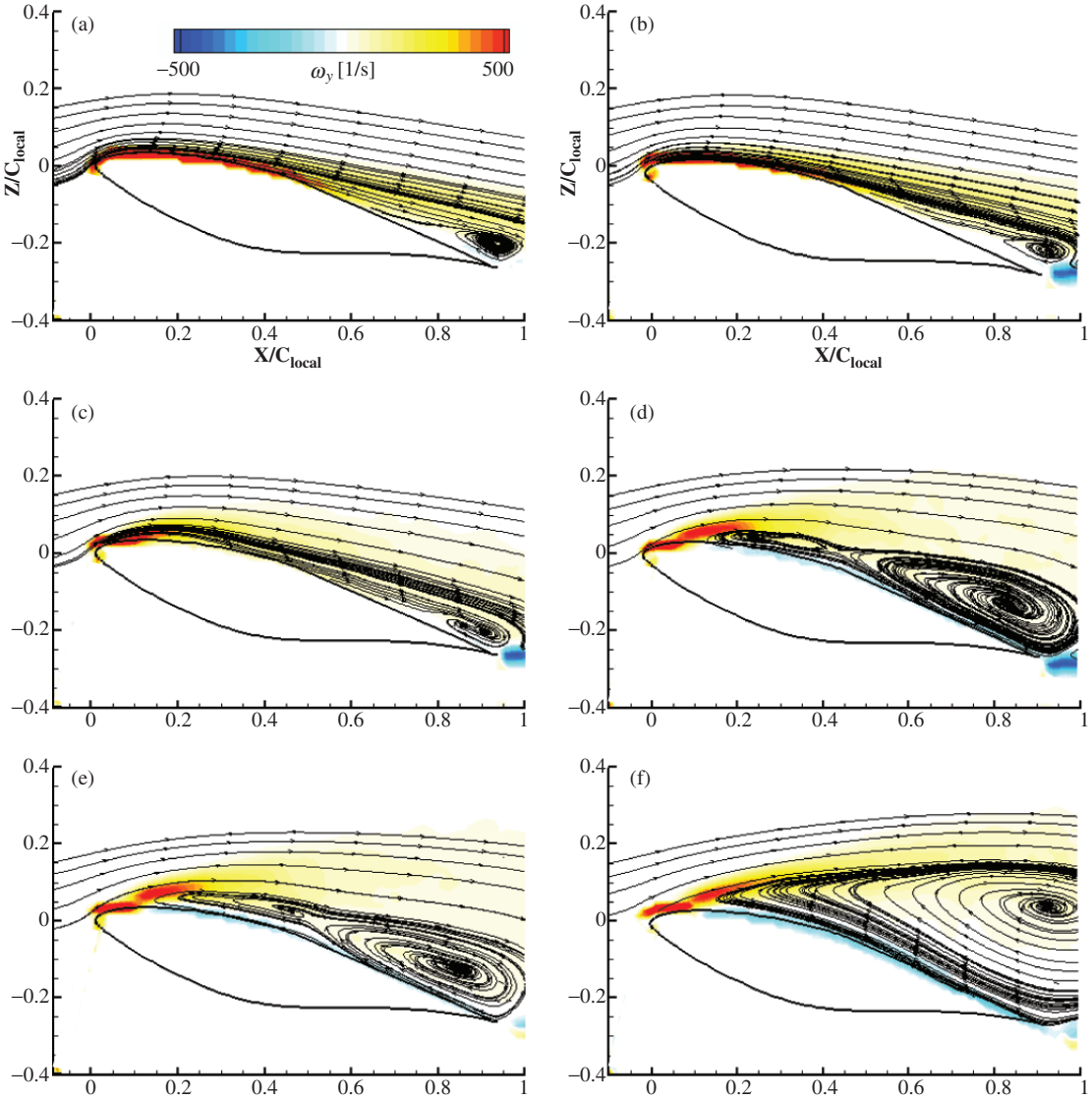

Figure 8. Superimposed spanwise vorticity and streamlines for the baseline case at y/b = 0.47 and Re = 1.85 × 10^5. α = 15° (a), 15.5° (b), 16° (c), 16.5° (d), 17° (e), and 17.5∞ (*f*)

When flow control is applied (Figure 9) the flow field at α = 15° and 15.5° (Figures 9a and b, respectively) is very similar to the baseline; thus, the minimal effect on the tip vibrations at these angles of attack, seen in Figure 7. However, as the angle of attack increases, the degree of flow separation is significantly reduced when flow control is applied (Figures 9c-f). These results qualitatively help explaining the trends in Figure 7, where the RMS of tip deflection stays almost constant for the forced case up to α = 16.5°, while for the baseline case there is a sharp increase in RMS values. This is directly

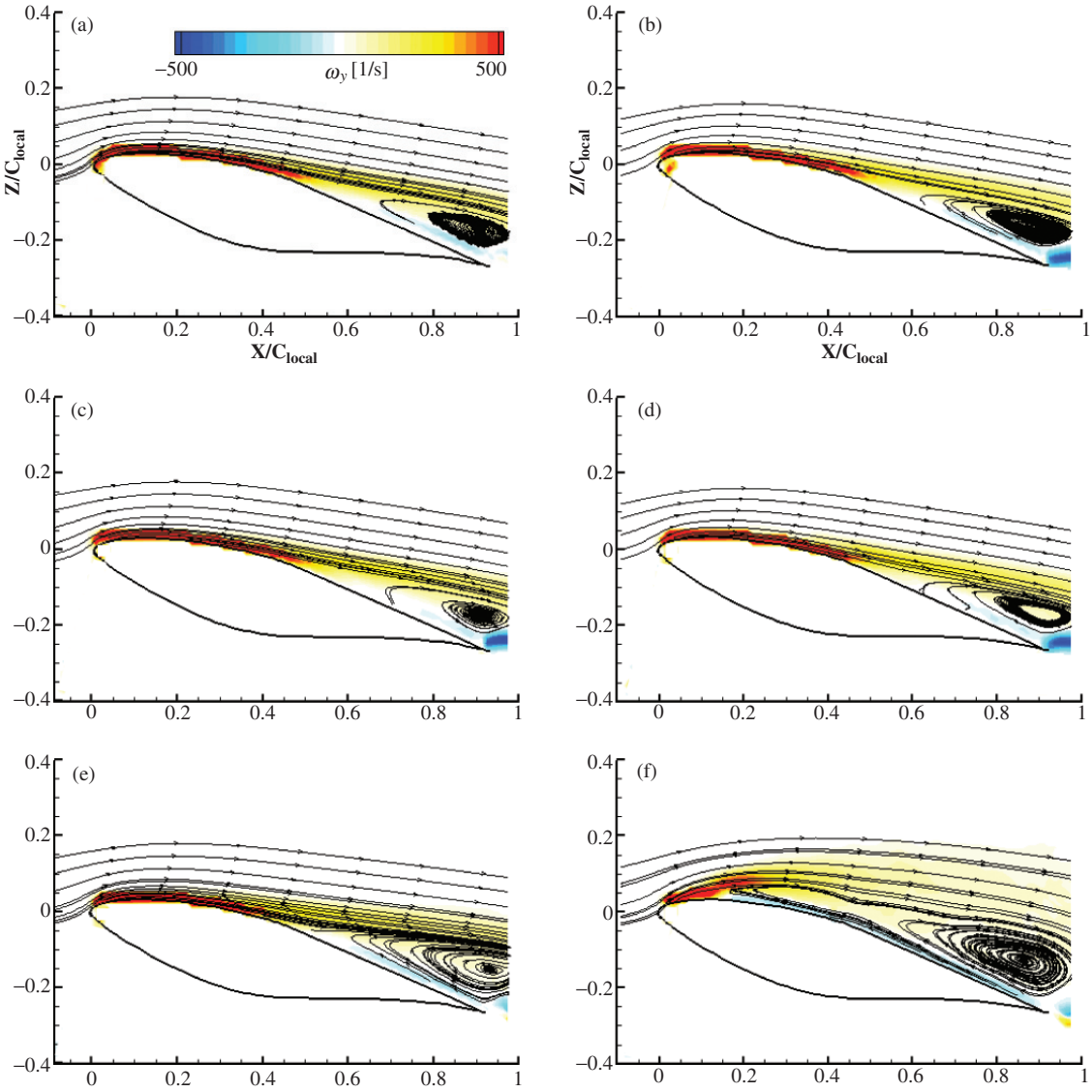

Figure 9. Superimposed spanwise vorticity and streamlines for the forced case at y/b = 0.47 and *Re* = 1.85×10^5. α = 15° (a), 15.5° (b), 16° (c), 16.5° (d), 17° (e), and 17.5° (f)

related to the extent and severity of the flow separation and reattachment. At higher angles of attack (i.e. α = 17° and 17.5°, Figures 9e and f, respectively), flow control is able to significantly reduce the flow separation. The result at α = 17.5° somewhat contradicts the small effect of flow control on the tip deflection (Figure 7) and needs to be further explored. Still, it is reasonable to conclude that the reduction in the extent of flow separation is predominantly responsible for reducing structural vibration of the blade.

4. SUMMARY AND CONCLUSIONS

The implementation of a synthetic jet based flow control system for a small-scale wind turbine blade model was presented, and the reduction of structural vibration reduction was measured for static blade pitch conditions. Flow control effectiveness was investigated in a wind tunnel at a range of Reynolds numbers and angles of attack (α = 15° to 17.5°). The effect of varying synthetic jet momentum coefficient, C_μ, and spanwise location of actuation were investigated at α = 16.5°. Increasing C_μ generally results in a decrease in the RMS tip deflection. Furthermore, the most effective spanwise location of the synthetic jets is near the tip. Also, when flow control was used, the magnitude of the PSD peak (at the structural frequency, f_{struc}) was shown to decrease by an order of magnitude

compared to the baseline case. Global flow field measurements were also acquired using the PIV technique at a spanwise location of $y/b = 0.47$ and for angles of attack from 15° to 17.5°. The largest effectiveness in flow re-attachment, and thus in vibrations reduction, was observed at $\alpha = 16.5°$.

ACKNOWLEDGEMENTS

This work was supported by the New York State Energy Research and Development Authority (NYSERDA), monitored by Mr. Michael Razanousky under PON1105.

REFERENCES

[1] D.T. Yen, C.P. van Dam, R.L. Smith, and S.D. Collins, *Active load control for wind turbine blades using MEM translational tabs,* 39th AIAA / ASME, 2001.

[2] D.T.Y Nakafuji, C.P. van Dam, J. Michel, and P. Morrison, *Load control for wind turbines – a non-traditional microtab approach,* 40th, AIAA / ASME, 2002.

[3] J.P. Baker, K.J. Standish, and C.P. van Dam, *Two-dimensional wind tunnel and computational investigation of a microtab modified S809 airfoil,* 43rd AIAA / ASME, 2005.

[4] R. Chow, and C.P. van Dam, *Computational investigations of deploying load control microtabs on a wind turbine airfoil,* 45th AIAA / ASME, 2007.

[5] A. W. Hulskamp, A. Beukers, H. Bersee, J.W. van Wingerden, and T.K. Barlas, *Design of a wind tunnel scale model of an adaptive wind turbine blade for active aerodynamic load control experiments,* 16th ICCM, 2007.

[6] S. Joncas, O. Bergsma, A. Beukers, *Power regulation and optimization of offshore wind turbines through trailing edge flap control, 2005* ASME Wind Energy Simposium, 2005.

[7] N. Troldborg, *Computational study of the Riso-B1-18 airfoil with a hinged flap providing variable trailing edge geometry, Wind Engineering,* 2005, 29, 89–113.

[8] P.B. Andersen, M. Guanaa, C. Bak, T. Buhl, *Load alleviation on wind turbine blades using variable airfoil geometry*, European Wind Energy Conference, Athens, 2006.

[9] S. Basualdo, *Load alleviation on wind turbine blades using variable airfoil geometry*, *Wind Engineering,* 2005, 29, 169–182.

[10] C. Bak, M. Gaunaa, P.B. Andersen, T. Buhl, P. Hansen, K. Clemmensen, R. Moeller, *Wind tunnel test on wind turbine airfoil with adaptive trailing edge geometry*, 45th AIAA Aerospace Sciences Meeting and Exhibit, Reno, 2007.

[11] M. Gaunaa, *Unsteady 2D potential-flow forces on a thin variable geometry airfoil undergoing arbitrary motion*, Technical Report Risø-R-1478(EN), Risø, 2006.

[12] T. Buhl, M. Gaunaa, C. Bak, *Potential of load reduction using airfoils with variable trailing edge geometry*, *J. Solar Energy Engineering,* 2005, 127, 503–516.

[13] J.R. Zayas, C.P. van Dam, R. Chow, J.P. Baker, E.A. Mayda, *Active aerodynamic load control for wind turbine blades*, European Wind Energy Conference, Athens, 2006.

[14] V. Maldonado, J. Farnsworth, W. Gressick, and M. Amitay, *Active control of flow separation and structural vibrations of wind turbine blades, Wind Energy*, Accepted, 2009.

[15] D. Oster, I.J. Wygnanski, *The forced mixing layer between parallel streams*, *J. Fluid Mechanics,* 1982, 123, 91–130.

[16] F.A. Roberts, *Effects of periodic disturbances on structure of mixing in turbulent shear layers and wakes*, PhD Thesis, California Institute of Technology, 1985.

[17] A. Seifert, T. Bachar, D. Koss, M. Shepshelovich, I. Wygnanski, *Oscillatory blowing: A tool to delay boundary-layer separation, AIAA Journal,* 1993, 31(11), 2052–2060.

[18] K.H. Ahuja, R.H. Burrin, *Control of flow separation by sound*, 9th AIAA / NASA Aeroacoustics Conference, 1984, Williamsburg, Virginia, AIAA-84-2298.

[19] D. Neuberger, I. Wygnanski, *The use of a vibrating ribbon to delay separation on two dimensional airfoils*, Air Force Academy Workshop in Unsteady Separated Flows, 1987, Colorado Springs, CO.

[20] A. Seifert, T. Bachar, D. Koss, M. Shepshelovich, I. Wygnanski, *Oscillatory blowing: A tool to delay boundary-layer separation*, *AIAA Journal,* 1993, 31(11), 2052–2060.

[21] I. Wygnanski, *Some observations affecting the control of separation by periodic excitation*, AIAA paper, 2000, 2314.

[22] M. Amitay, A. Glezer, *Role of actuation frequency in controlled flow reattachment over a stalled airfoil*, *AIAA Journal*, 2002, 40, 209–216.

[23] M. Amitay, M. Horvath, M. Michaux, A. Glezer, *Virtual aerodynamic shape modification at low angles of attack using synthetic jet actuators*, AIAA Paper, 2001, 2975.

[24] M. Amitay, A. Glezer, *Controlled transients of flow reattachment over stalled airfoils*, *Int. J. of Heat Transfer and Fluid Flow,* 2002, 23, 690–699.

[25] M. Amitay, A. Glezer, *Flow transients induced on a 2-D airfoil by pulse-modulation actuation*, *Experiments in Fluids*, 2006, 40, 329–331.

[26] M. Amitay, D.R. Smith, V. Kibens, D.E. Parekh, A. Glezer, *Modification of the aerodynamics characteristics of an unconventional airfoil using synthetic jet actuators*, AIAA Journal, 2001, 39, 361–370.

[27] M.E. Desalvo, A. Glezer, *Control of airfoil aerodynamic performance using distributed trapped vorticity*, 45th AIAA Aerospace Sciences Meeting and Exhibit, 2007.